300 GHz Broadband Transceiver Design for Low-THz Band Wireless Communications in Indoor Internet of Things

Nabil Khalid, Naveed A. Abbasi and Ozgur B. Akan
Next-generation and Wireless Communications Laboratory
Department of Electrical and Electronics Engineering
Koc University, Istanbul, Turkey
Email: {nkhalid15, nabbasi13, akan}@ku.edu.tr

***Abstract*—This paper presents the architectural design of a 300 GHz transceiver system that can be used to explore the high speed communication opportunities offered by the Terahertz (THz) band for advanced applications of Internet-of-Things (IoT). We use low cost industry ready components to prepare a fully customizable THz band communication system that provides a bandwidth of 20 GHz that is easily extendable up to 40 GHz. Component parameters are carefully observed and used in simulations to predict the system performance while the compatibility of different components is ensured to produce a reliable design. Our results show that the receiver provides a conversion gain of 51 dB with a noise figure (NF) of 9.56 dB to achieve a data rate of 90.31 Gbps at an operation range of 2 meters, which is suitable for high speed indoor IoT nodes. The flexible design of the transceiver provides groundwork for further research efforts in 5G IoT applications and pushing boundaries of throughputs to the order of terabits per second (Tbps).**

***Index Terms*—Link budget analysis, transceiver design, 5G indoor wireless networks, 300 GHz band, Internet-of-Things (IoT) links, Terahertz (THz) communication.**

I. Introduction

The Internet is now ubiquitous and widely used for applications like information transfer, social networking, banking and online shopping. Emerging applications of IoT require information sharing technologies that connect smart machines to the Internet along with people. Such applications of IoT are expected to transform our world from household life to modern businesses [1]. Many IoT applications such as video surveillance, ultra-high-definition UHD displays and wireless back haul demand high data rates that are expected to increase further. In order to develop the technologies to satisfy consumer needs, 5G wireless networks need to realize data rates reaching terabits per second (Tbps) [2]. The 60 GHz spectrum is expected to increase data rates up to 6 Gbps [3], however, the available spectrum around this frequency is limited to only 9 GHz, which may not be able to completely satisfy the high data rate demands. Therefore, there is a lot of interest in exploring THz band communications (0.3 - 10 THz). This motivates the implementation of transmission and reception frontends for THz band that operate above 300 GHz.

Higher frequencies can support higher data rates, however, being highly directional, they are more easily blocked by obstacles on their path. This provides a unique set of challenges for THz band communications. To overcome these problems, THz band equipment is constantly improving performance with current research activities. The experimental THz band equipment can be categorized mainly into two groups depending on the approach for generating THz band signals. In a top-down approach, photonics technology is used to achieve communication that is translated from electronic to optical frequencies, while in a bottom-up approach, the operating frequency of electronics components is increased to the order of THz [4]. The bottom-up approach is a preferred course for consumer designs because optical components are more expensive than silicon components used in the bottom-up approach. Apart from cost, the size of silicon-based components is also more compact. Commonly used THz band experimental setups are based on bottom-up approach involving subharmonic Schottky diode mixers [5], [6].

The bottleneck of THz band communication is the technology supporting it, and thus, there is an enormous need to explore different techniques as potential candidates. As discussed earlier, encouraging results for THz band are demonstrated using frontends based on photonic and electronic technologies. Using a 250 nm Indium Phosphide (InP) double heterojunction bipolar transistor (DHBT), [7] shows the transmission of 48 Gbps using 64-QAM/QPSK Direct-Conversion Transceiver Chipset. In [8], a 40 nm CMOS transmitter is presented that uses 32-QAM to provide 17.5 Gbps per channel capability over six channels. A Gallium Arsenide GaAs-based 35nm metamorphic high electron mobility transistor (mHEMT) integrated transmitter and receiver designed using Monolithic Microwave Integrated Circuits (MMIC) is shown to provide a 64 gigabits per second (Gbps) point-to-point link at 300 GHz for a distance of 2 meters in [9]. Although MMIC based designs are more robust from a manufacturing perspective, their in-flexibility and lack of customization makes them unsuitable for research efforts where a number of system parameters need to be optimized. Whereas for experimentation purposes, it is very important that the system customizable such that a single component block can be easily replaced or modified, unlike the case with MMICs.

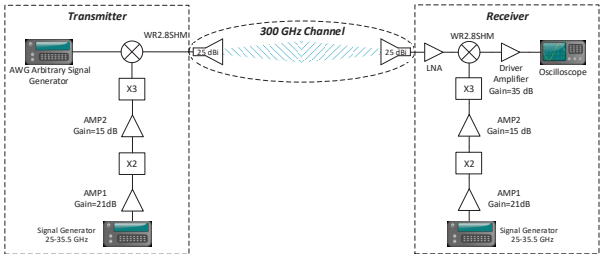

Fig. 1: Simplified block diagram of the THz band transmitter and receiver.

Therefore, in this work, we provide a fully customizable transceiver design that is capable of operating with a 20 GHz bandwidth. The design uses state-of-the-art discrete components such as WR2.8 subharmonic mixer (SHM) to operate in THz band. Full transceiver design is discussed and simulations based on the components characteristics are performed to achieve first pass success. The results for single-tone analysis, two-tone analysis, phase noise, receiver noise and receiver gain are discussed. Simulation results show that the transceiver operates reliably at 2 meters and provides data rates of up to 90.31 Gbps. The transceiver design can be further modified with ease to operate with a 40 GHz bandwidth.

The remainder of this paper is organized as follows. In Section II, we discuss the design and selection of components for the transceiver. Section III describes the simulation results for the first pass success of our design. Finally, we conclude the paper in Section IV.

II. Transceiver Design

To achieve high throughput from the bandwidth available in the THz band, an ultra-wideband frontend is required. The huge path loss in the band limits communication distances to only a few meters and also requires highly directive antennas to transmit the limited power generated from solid-state electronics. Therefore, during the design of the transceiver, our goal is to select ultra-wideband components that would provide at least 20 GHz of bandwidth and operate for a minimum distance of 2 meters.

To get an estimate of the characteristics of the required components, we first calculate noise floor values and the expected channel path loss for 20 GHz Bandwidth and a 2 meters channel length. The Jhonson noise power for a bandwidth (B) of 20 GHz in a wideband channel is calculated as -79.96 dBm using,

$$N_R = 10 \cdot \log_(\frac{kTB}{10^{-3}}), \quad (1)$$

where, $k = 1.38 \times 10^{-23}$ J/K is Boltzmann's constant and T is the noise temperature in Kelvin. To predict the path loss, we use the free space path loss (FSPL) expression given as,

$$FSPL = 20\log(d) + 20\log(f) + 20\log\left(\frac{4\pi}{c}\right), \quad (2)$$

where, d is distance in meters and f is frequency in Hz. For a distance of 2 meters and a frequency of 300 GHz, the

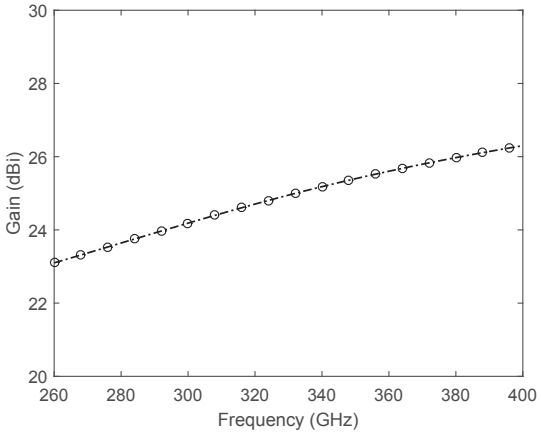

Fig. 2: Antenna gain 260 GHz to 400 GHz range.

$FSPL$ is 88 dB. This dictates that either we provide high output power at the transmitter or use components that can overcome the path loss. For the first option, if we consider a margin of 15 dB (10 dB receiver NF and 5 dB for antenna misalignment), the minimum detectable signal at the receiver would be -64.96 dBm and this suggests that the output power of the transmitter must be higher than $+23.04$ dBm (provided 88 dB FSPL), which is not a good choice because of its high value. Alternatively, a benefit of high frequency is a small effective aperture that can provide high gain. This is because antenna gain is inversely proportional to the wavelength [10]. Hence, in our design we prefer using high gain antennas at the transmitter and the receiver along with state-of-the-art components that minimize receiver noise floor. A simplified block diagram of our design in shown in Fig. 1. In a typical transceiver, a transmitter and receiver are housed together.

A. Receiver

We now discuss the components selected in our receiver design based on the requirements discussed in the preceding sections.

1) Antenna: The significantly high loss at THz Frequency is fortunately overcome by the small sized high gain antennas [11]. The antennas used in our design is a pyramidal horn antenna with gain of 25 dBi and horn length of 21.4 mm. Whereas at the lowest frequency (260 GHz) it is 2 dB lesser and at the highest frequency (400 GHz) it is 1.5 dB higher. The half power beamwidth is 12°. The gain of our antenna, from 260 to 400 GHz, is shown in Fig. 2.

2) Low Noise Amplifier: The receiver requires high sensitivity, which is typically influenced by its initial components and hence there should be minimal thermal losses at the input. Low noise amplifiers are designed to meet this criterion by matching the transistor's input for optimum NF while the output is conjugately matched to the system impedance (usually 50 ohms) for maximum gain and return loss. For a robust production, a low noise amplifier is usually designed using a transistor model and it is sufficient to use a linear

TABLE I: Local oscillator single-sideband phase noise.

Frequency Range	10 Hz	100 Hz	1 kHz	10 kHz	100 kHz	1 MHz
20 to 40 GHz	-48 dBc	-72 dBc	-94 dBc	-100 dBc	-100 dBc	-124 dBc
40 to 67 GHz	-42 dBc	-66 dBc	-88 dBc	-94 dBc	-91 dBc	-118 dBc

model [12]. The noise input power is modeled by a resistor where its thermal agitation acts as noise [13]. Transistor technology selection is a critical parameter and for low noise devices, pseudomorphic HEMT (pHEMT) is the most popular technology due to its low NF and high gain, however, at the expense of cost. mHEMT, on the other hand, combines performance of the pHEMTs and affordability of GaAs process. Therefore, the transceiver design is based on InAlAs/InGaAs based mHEMT technology fabricated by a 35 nm process. Initial design of the LNA is discussed in [14] and an improved version that provides small signal gain of 25 dB from 220 to 325 GHz with a NF of 7.2 dB is described in [9].

3) Mixer: To process the information in the modulated signal, it is necessary to down convert the signal to a band that can be digitized and processed easily. Heterodyne receivers that employ a mixer which multiplies the two input signals, namely the RF and the local oscillator (LO), and outputs the sum or difference intermediate frequencies (IF) are commonly used in such cases. For communication in 300 GHz band, the required LO signal needs to be at very high frequency, however, due to the cost and difficulty of providing high frequency LO signal, subharmonic types of mixers are generally used that require N times smaller LO frequency (where $N \geq 2$).

Usually planar Schottky diodes are preferred as they exhibit better reproducibility, operation at room temperature and enable the integration of several diodes in balanced or anti-parallel configurations [15], [16]. Hence the mixer used in our system is WR2.8SHM by Virginia diodes, that operates in 260 to 400 GHz band with an LO input frequency of 130 to 220 GHz. The mixer exhibits double side band (DSB) equivalent noise temperature between 800 and 1500 Kelvin. We calculate the mixer NF using $NF = 10log(1+T_e/T_0)$. Where T_e is the equivalent noise temperature and T_0 is the room temperature (290 K). Considering 1000 K equivalent noise temperature in the required band, this comes out to be 6.48 dB. With a 3 to 6 dBm of LO power, typical DSB conversion loss is 9 dB and optimal IF input power is -10 dBm. A DSB type mixer is used without any input image rejection and thus both bands are equally propagated.

4) LO Signal: The LO signal of the mixer is the driver signal that has a switching impact. The drive power level has direct impact on the performance of the mixer. Since the selected mixer, WR2.8SHM is a subharmonic mixer, the required LO frequency is from 130 to 200 GHz with a power range of 3~6 dBm. To generate such a high frequency signal with considerable power, we designed a multiplier amplifier chain (Fig. 1) where required input signal frequency range is 25 to 35.5 GHz. This signal can be easily generated using any available frequency synthesizer with low phase noise. For this purpose we used, MG3690C by Anritsu whose output power is up to $+6$ dBm and phase noise characteristics are given in the Table I [17]. The generated signal is then amplified using Ka band ERZ-HPA-2300-3700-27 power amplifier by ERZIA, which is shown as AMP1 in Fig. 1. The saturation power of the amplifier is 27 dBm and the gain is 21 dB. The output of the amplifier is fed to the frequency doubler, SFP-152KF-S1. Since this is a passive X2 frequency multiplier, the required input power is very high but can be provided by the amplifier preceding this multiplier.

The output signal frequency of the multiplier is 50 to 75 GHz provided by WR-15 waveguide with the output power of $+5$ dBm. Before further multiplication, this signal is amplified using QPW50662315 power amplifier by QuinStar Technology Inc, shown as AMP2 in Fig. 1. It operates from 50 to 66 GHz and provides a gain of 15 dB with 1 dB compression point at 23 dBm. The signal after amplification is fed to passive X3 frequency multiplier WR5.1x3HP by Virginia diodes Inc, that has 3% efficiency. The input signal power should be at least 18 dBm to compensate for the multiplier losses of approximately 15 dB and thus provide the LO signal to the mixer with the required minimal power. This output is fed to the LO port of WR2.8SHM mixer.

5) Driver Amplifier: The IF signal generated by the mixer is a down-converted signal that is amplified before digitization for better receiver gain. The amplifier used is DBLNA500013000A from DBWave Technologies, that operates from 0.01 to 30 GHz range with the NF of 4.5 dB. The gain of the amplifier is 35 dB with a 1 dB compression point at 28 dBm.

The signal generated at the amplifier's output is ultra-wideband and to capture the signal we used state-of-the-art real-time oscilloscope (RTO) DPO72304SX by Tektronics, that features sampling rate of 100 GSps with an analog bandwidth of 23 GHz.

B. Transmitter

The block diagram of transmitter is shown in Fig. 1. The LO signal generation for the transmitter is same as the receiver. RF path power amplifier is not used in the design for simplicity and because of the fact that the link is being designed for short distances. High speed signal generation is an intricate issue and it is resolved by using state-of-the-art M8195A 65 GSaps Arbitrary Waveform Generator from Keysight that provides analog signal bandwidth up to 25 GHz.

The saturation power of the WR2.8SHM is -10 dBm and hence the IF port power is limited to this value. Due to 9 dB mixer conversion loss, the maximum output power of the mixer is calculated as -19 dBm. To overcome high path loss, antennas used in our design are 25 dBi each at the transmitter and the receiver.

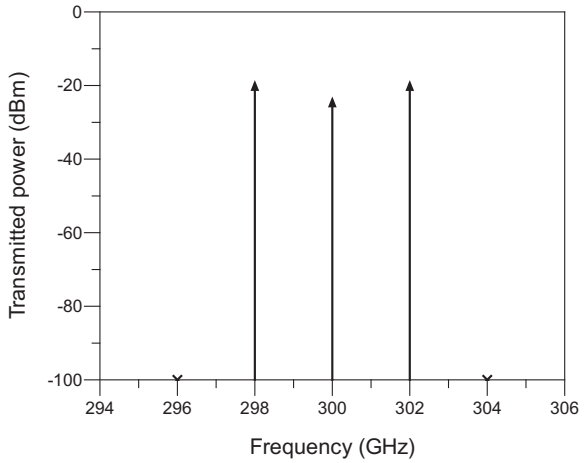

Fig. 3: Output spectrum of the 300 GHz band transmitter.

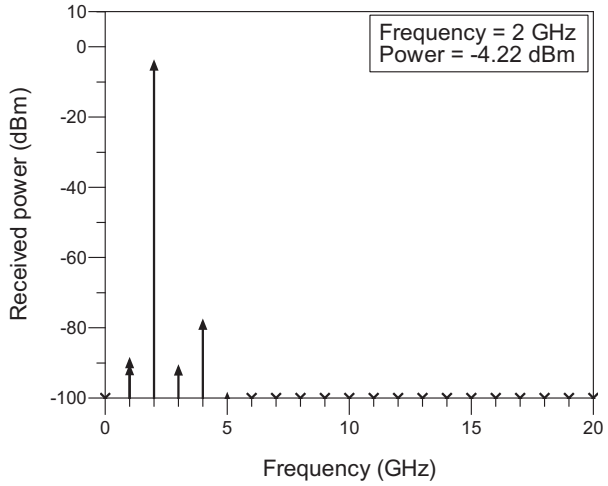

Fig. 4: Baseband output spectrum of the receiver when excited by the DSB signal.

III. Results

To ensure first pass success of our design, we performed necessary system design simulations to evaluate the transmitter and the receiver. The lower limits for the effectiveness of a system are established by the noise. In principal, three main parameters that establish the performance of a wireless link are: dynamic range, sensitivity and selectivity. The first two are dictated by the receiver NF and linearity characteristics while selectivity is dictated by the phase noise contribution by the oscillator [18]. The linearity performance of the receiver is determined by performing single-tone and two-tone analysis. To analyze selectivity, we perform single sideband phase noise measurements and discuss our results. Finally, we show the receiver gain and the NF of the receiver.

A. Single-Tone Analysis

In this analysis, the performance of the proposed transceiver is analyzed for a single-tone input signal. We apply a 2 GHz signal with -10 dBm power to the IF port of the WR2.8SHM mixer. This analysis measures the power signal spectrum at the output of mixer. Due to the DSB nature of the mixer, the output spectrum contains the upper sideband signal of 302 GHz and lower side band signal of 298 GHz with output power of -19.114 dBm each, as shown in Fig. 3. The carrier frequency of 300 GHz can also be seen with output power of -23.58 dBm. This signal is passed through a channel model where at a distance of 2 m provides 38 dB of pathloss (considering antenna gain of 25 dBi each at Tx and Rx).

The transmitted signal is then fed to the receiver and is downconverted by the mixer after amplification. This baseband signal is amplified using a driver amplifier and the output spectrum is shown in Fig. 4. This signal is fed to the high sampling rate oscilloscope for signal processing. Several mixing products are observed in the baseband spectrum, however, the highest spurious signal is at least 60 dB below the required signal, which is much higher than the rule of thumb of 30 dBc and hence can be ignored.

B. Two-Tone Analysis

Non-linearity in the transfer function of receiver can be problematic for the communication system as the modulated signal is distorted causing difficulty in information retrieval. One of the main contributors that cause non-linearity are the amplifiers because when the device enters its compression region, the non-linear effects start to become apparent [19]. Two-tone analysis is a popular technique in which non-linearity of the circuit is determined by finding the carrier to intermodulation ratio (C/I) that is defined as the ratio of useful component output power to the intermodulation distortion (IMD) output power [13]. In this technique, more than one carrier frequency with slight frequency spacing are applied to the circuit resulting in multiple sidebands due to the mixing that is introduced by the non-linear behavior of the device. Usually third order intermodulation products ($IM3$) appearing at $2f_1 - f_2$ and $2f_2 - f_1$ are the major source of distortion and are sufficient to predict the device performance.

$IM3$ of the proposed receiver is analyzed by applying input signals centered at 302 GHz with tone spacing (Δf) 2 MHz and calculating the ratio of intermodulation products and the carrier given by the following equation,

$$IM3(dBc) = 10\log\left(\frac{P_{2f_2-f_1}}{P_{f_2}}\right) = 10\log\left(\frac{P_{2f_1-f_2}}{P_{f_1}}\right), \quad (3)$$

The output spectrum of the receiver, when excited by two input signals of -32.5 dBm with tone spacing (Δf) 2 MHz, is shown in Fig. 5. The calculated C/I with these conditions is -30.69 dBc. This shows that our proposed transceiver design enters into non-linear region for an input power greater than -29.5 dBm that appears for inter-transmitter-receiver distances smaller than 8 cm.

C. Phase Noise Analysis

Phase noise is a key parameter in determining the minimum frequency spacing required in between adjacent channels. It is

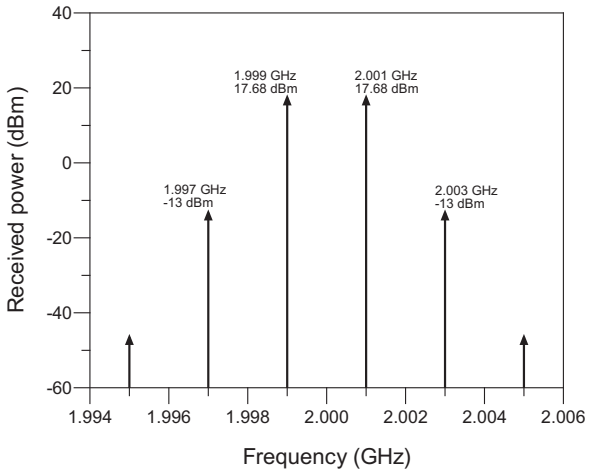

Fig. 5: Baseband output spectrum of the receiver when excited by a two-tone input signal of -32.5 dBm.

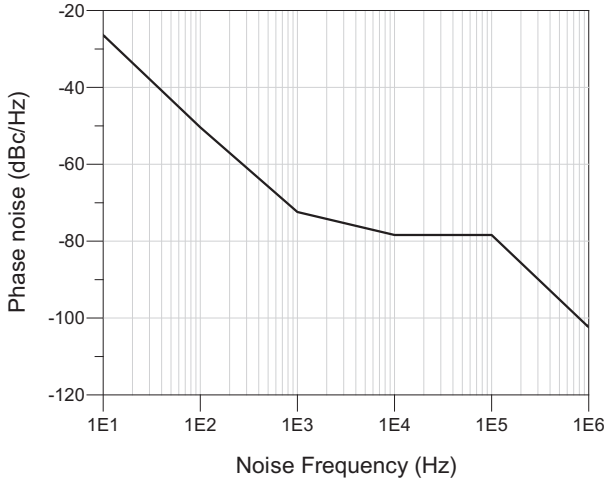

Fig. 6: Phase noise of the receiver determined at the output of the driver amplifier.

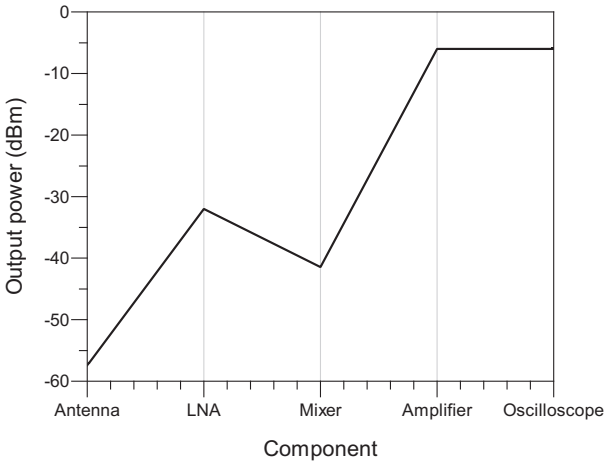

Fig. 7: Output power of each component when the receiver is excited by -57 dBm signal power.

primely generated by the signal generator, which is usually low for highly stable signal synthesizers, however, the amplifiers in the system might increase the phase noise leading to performance degradation. To get an insight of the selectivity of our receiver, we performed phase noise analysis. The results in Fig. 6 shows that the phase noise initially decreases with the slope of 30 dB/decade and after 100 KHz, it gets below -80 dBc. To illustrate this further, consider an example in which received power is -57 dBm at distance of 2 meters, while the noise floor of the receiver is -79.96 dBm. The signal to noise ratio for this particular example is calculated as 22.96 dB. On the other hand, it can be seen from the Fig. 6 that, at 10 Hz offset from the carrier, the phase noise is 27 dB below the carrier. Thus, for this particular case, the adjacent channel separation is suggested to be at least 10 Hz. However, for better compatibility, the recommended separation is 100 KHz. This separation will ensure that the interference in adjacent channels remain minimum.

D. Receiver Gain and Noise Figure

Another important parameter to determine is the overall receiver gain and NF. This helps in determining the minimum detectable signal by a receiver. Based on the gain, loss and compression of components in the receiver chain, ratio of output power to the input power is calculated to determine the receiver gain. The NF of the system is calculated based on the NF and gain of each component. It should be noted here that the NF is dominated by the first few components in the chain and once the desired signal is amplified well above the noise of the following components, their impact in increasing the signal noise is minimized. Results in Fig. 7 and Fig. 8 show that the receiver gain is higher than 51 dB whereas the NF is 9.56 dB, respectively. The receiver gain results are shown for an inter-transmitter-receiver distance of 2 m. This suggests that the minimum detectable signal for our receiver is -70.4 dBm. Hence for the distance of 2 m, the receiver signal to noise ratio is 13.4 dB. Using Shannon's capacity formula, we determine the capacity of the proposed system as 90.31 Gbps. The link budget is summarized in Table II. While the performance comparison of our system is shown in Table III.

IV. Conclusion

In this paper, we propose a broadband transceiver design for 300 GHz band wireless communication based on discrete components that may be used in future IoT applications. We use low cost industry ready components that can be easily modified based on application specific requirements. The proposed transceiver provides a bandwidth of 20 GHz making it a good candidate for exploring wide band channel capabilities around the 300 GHz frequency band for 5G applications of IoT. Component parameters are used to simulate the system design to ensure first pass success. Linearity, noise and selectivity characteristics of the system are analyzed based on single-tone, two-tone, receiver gain, noise figure, and phase

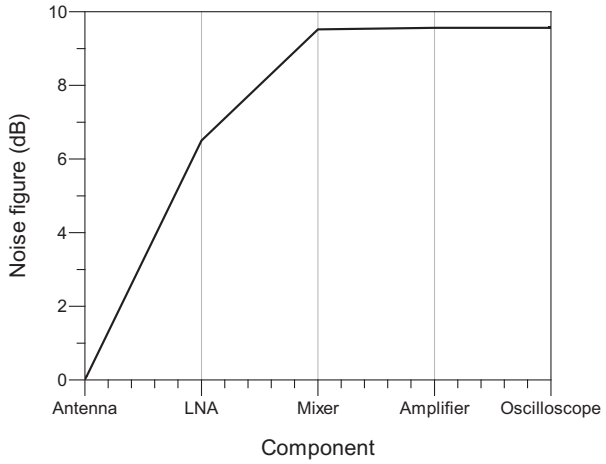

Fig. 8: Noise figure of the receiver determined based on the noise and gain contribution of each component.

TABLE II: Link budget.

Parameter	Unit	Value
Start frequency	GHz	300
Stop frequency	GHz	320
Bandwidth	GHz	20
RF Tx Power	dBm	-19
Tx and Rx antenna gain	dBi	25
Link Distance	m	2
FSPL	dB	88
Rx LNA input power	dBm	-57
System temperature	K	290
Mixer noise temperature	K	1000
Rx noise figure	dB	9.56
Receiver gain	dB	51
Minimum detectable signal	dBm	-70.4
IM3 of the receiver	dBm	-29.5
SNR @ 2 m	dB	13.4
Max Range @ SNR = 10 dB	m	2.9

TABLE III: Performance comparison of the proposed system.

Parameter	This work	[7]	[8]	[9]
Bandwidth SSB (GHz)	20	17	4.7	32
Output power (dBm)	-19	9	-14.5	-4
Antenna gain (dBi)	25	40	-	24.2
Receiver noise figure (dB)	9.56	9.5	-	6.7
Link distance (m)	2.9	1.8	-	2.4

noise analysis, which provides detailed insight of our proposed system. Finally, it is shown that our system is capable of providing 90.31 Gbps data throughput at 2 m. Future work includes analysis of digital data transmission on the proposed transceiver to determine practically achievable data rates.

V. Acknowledgment

This work was supported in part by the Scientific and Technological Research Council of Turkey (TUBITAK) under grant $\#113E962$.

References

[1] C. X. Mavromoustakis, G. Mastorakis, and J. M. Batalla, *Internet of Things (IoT) in 5G Mobile Technologies*. Springer, 2016, vol. 8.

[2] K.-C. Huang and Z. Wang, "Terahertz Terabit Wireless Communication," *Microwave Magazine, IEEE*, vol. 12, no. 4, pp. 108–116, June 2011.

[3] IEEE, "Part 15.3: Wireless Medium Access Control and Physical Layer Specifications for High Rate Wireless Personal Area Networks," *IEEE*, 2009.

[4] R. Piesiewicz, T. Kleine-Ostmann, N. Krumbholz, D. Mittleman, M. Koch, J. Schoebei, and T. Kurner, "Short-Range Ultra-Broadband Terahertz Communications: Concepts and Perspectives," *IEEE Antennas and Propagation Magazine*, vol. 49, no. 6, pp. 24–39, Dec 2007.

[5] N. Khalid and O. B. Akan, "Wideband THz communication channel measurements for 5G indoor wireless networks," in *2016 IEEE International Conference on Communications (ICC)*, May 2016, pp. 1–6.

[6] ——, "Experimental Throughput Analysis of Low-THz MIMO Communication Channel in 5G Wireless Networks," *IEEE Wireless Communications Letters*, vol. PP, no. 99, pp. 1–1, 2016.

[7] S. Carpenter, D. Nopchinda, M. Abbasi, Z. S. He, M. Bao, T. Eriksson, and H. Zirath, "A D -Band 48-Gbit/s 64-QAM/QPSK Direct-Conversion I/Q Transceiver Chipset," *IEEE Transactions on Microwave Theory and Techniques*, vol. 64, no. 4, pp. 1285–1296, April 2016.

[8] K. Katayama, K. Takano, S. Amakawa, S. Hara, A. Kasamatsu, K. Mizuno, K. Takahashi, T. Yoshida, and M. Fujishima, "A 300 GHz CMOS Transmitter With 32-QAM 17.5 Gb/s/ch Capability Over Six Channels," *IEEE Journal of Solid-State Circuits*, vol. PP, no. 99, pp. 1–12, 2016.

[9] I. Kallfass, D. Iulia, R. Sebastian, P. Harati, J. Antes, A. Tessmann, S. Wagner, K. Michael, R. Weber, H. Massler *et al.*, "Towards MMIC-Based 300GHz Indoor Wireless Communication Systems," *IEICE Transactions on Electronics*, vol. 98, no. 12, pp. 1081–1090, 2015.

[10] C. Balanis, *Antenna Theory: Analysis and Design*. Wiley, 2016.

[11] J. F. Johansson and N. D. Whyborn, "The diagonal horn as a submillimeter wave antenna," *IEEE Transactions on Microwave Theory and Techniques*, vol. 40, no. 5, pp. 795–800, May 1992.

[12] P. Huang, R. Lai, R. Grundbacher, and B. Gorospe, "A 20-mW G-band Monolithic Driver Amplifier Using 0.07- um InP HEMT," in *2006 IEEE MTT-S International Microwave Symposium Digest*, June 2006, pp. 806–809.

[13] I. Bahl, *Fundamentals of RF and Microwave Transistor Amplifiers*. Wiley, 2009.

[14] A. Tessmann, A. Leuther, H. Massler, M. Kuri, and R. Loesch, "A Metamorphic 220-320 GHz HEMT Amplifier MMIC," in *2008 IEEE Compound Semiconductor Integrated Circuits Symposium*, Oct 2008, pp. 1–4.

[15] L. Miao, J. Jiang, C. Wang, X. J. Deng, and B. Lu, "A 340GHz sub-harmonic mixer based on planar Schottky diodes," in *2014 39th International Conference on Infrared, Millimeter, and Terahertz waves (IRMMW-THz)*, Sept 2014, pp. 1–2.

[16] B. Thomas, A. Maestrini, and G. Beaudin, "A low-noise fixed-tuned 300-360-GHz sub-harmonic mixer using planar Schottky diodes," *IEEE Microwave and Wireless Components Letters*, vol. 15, no. 12, pp. 865–867, Dec 2005.

[17] *RF/Microwave Signal Generators MG3690C*, Anritsu, 2015.

[18] J. Laskar, B. Matinpour, and S. Chakraborty, *Modern Receiver Front-Ends: Systems, Circuits, and Integration*. Wiley, 2004.

[19] N. Khalid, T. Abbas, and M. B. Ihsan, "Power amplifier design using GaN HEMT in class-AB mode for LTE communication band," in *2015 International Wireless Communications and Mobile Computing Conference (IWCMC)*, Aug 2015, pp. 685–689.